Research Article

Nef Deletion in HIV-1$_{eli}$ Eliminates Peripheral CD4 T-Cell Loss in a Humanized BLT Mouse Model of HIV Disease

Clever JL*, Tam SM, Rold CJ, Strings VR, Wadekar S, Lira V, Fatehi E, Bansal N, Martin V and Apte S

ImmunoScience, Inc., 6670 Owens Drive, Pleasanton, CA 94588, USA

*Corresponding author: Jared L Clever, ImmunoScience, Inc., 6670 Owens Drive, Pleasanton, CA 94588, USA, Tel: 9254024209; E-mail: jared.clever@immunoscience.com

Abstract

Background: Humans infected with HIV-1 containing nef gene deletions show very slow or non-progression to AIDS. Therefore, a nef-deleted HIV-1 may be useful in generating a pathogenically-attenuated candidate therapeutic HIV-1 vaccine. We have created a mutant of HIV-1$_{eli}$ lacking a functional nef gene. In this study we have characterized the pathogenic phenotype of this mutant in an animal model of HIV-1 disease.

Methods and findings: We determined the contribution of the nef gene to replication and infectivity in cell culture and to pathogenesis in humanized BLT mice after infection with HIV-1$_{eli}$, a CXCR4-tropic subtype D virus. We constructed a nef-null virus to create HIV-1$_{eli\Delta nef}$. Human peripheral blood mononuclear cell cultures from 13 different donors were infected and viral growth was monitored for 14 days. HIV-1$_{eli}$ produced higher p24 levels compared to HIV-1$_{eli\Delta nef}$, indicating lower viral replication. HIV-1$_{eli}$ and HIV-1$_{eli\Delta nef}$ were then used to infect humanized BLT mice. Viremia was delayed several weeks in the HIV-1$_{eli\Delta nef}$-infected mice compared to HIV-1$_{eli}$. Viremia was evident in the majority of mice infected with HIV-1$_{eli}$ by 3 weeks post-infection while viremia was not evident in any HIV-1$_{eli\Delta nef}$ infected mice until 7 weeks post-infection. Mice infected with HIV-1$_{eli}$ harbored an average of 2.94e5 ± 1.6e5 copies of viral RNA/ml in blood. In contrast, blood from mice infected with HIV-1$_{eli\Delta nef}$ harbored an average of 4.4e3 ± 4.5e3 copies of viral RNA/ml; a ~1.5-log reduction in average viremia. Flow cytometry revealed that all mice infected with HIV-1$_{eli}$ showed a precipitous decline in the ratio of human CD4$^+$ to CD8$^+$ T-cells in peripheral blood from week 1 to week 7 post-infection. In sharp contrast, none of the mice infected with HIV-1$_{eli\Delta nef}$ showed a sustained decline of CD4$^+$ to CD8$^+$ T-cells from week 1 to week 10 post-infection.

Conclusions: We conclude that nef is necessary for high levels of viral replication both *in vitro* and *in vivo* and for depletion of peripheral CD4$^+$ T-cells in HIV-1$_{eli}$, a pathological hallmark of HIV-1 disease. We have generated and characterized a pathogenically-attenuated mutant of HIV-1$_{eli}$ lacking a functional nef gene in a humanized mouse model of HIV-1 disease.

Keywords: HIV/AIDS pathogenesis; HIV-replication; Animal models of HIV disease

Introduction

Nef is a multi-functional accessory protein encoded by primate lentiviruses. Nef is known to downregulate several surface proteins on infected cells including the HIV receptor CD4 [1,2], the HIV co-receptors CXCR4/CCR5 [2-4] and MHC class I molecules [2,5], among others (reviewed in [2,6]). Nef also activates several cellular protein kinase pathways [7,8]. In addition, nef significantly increases the infectivity of virion particles but the exact mechanism remains unclear [6,9,10]. *In vivo*, nef plays a crucial role in HIV-1 pathogenesis (reviewed in [11]). Nef is arguably the most important pathogenesis-associated accessory gene encoded by HIV-1. Evidence for this is the observation that several reported cases of humans infected with nef-defective HIV-1 isolates showed markedly delayed or non-progression to AIDS [12-17]. When HIV-1 nef was expressed alone in transgenic mice, it was shown to have direct pathogenic effects unlike any other HIV-1 protein [18]. The nef gene of SIV has also been extensively studied and shown to be necessary for normal progression to simian AIDS in rhesus macaques infected with SIVmac [19,20].

In this study we have determined the pathogenic contribution of nef using a subtype D HIV-1 strain, HIV$_{eli}$; which utilizes the T-cell tropic CXCR4 coreceptor for infection [21]. Humanized BLT mice offer an advanced animal model for studying HIV-1 pathogenesis as they are created by human stem cell engraftment in bone marrow along with human fetal liver/thymus implants (reviewed in [22,23]). These mice display a full range of human immune cells including monocytic cells, B cells, dendritic cells and T-cells which are disseminated throughout the animal [22,23].

We found that deletion of nef resulted in reduced infectivity of virus in cell culture and reduced replication in activated primary human peripheral blood mononuclear cells (PBMCs) compared to wildtype. In BLT mice, deletion of nef led to a delay in onset of viremia by several weeks and to reduced viral loads up to 10 weeks post-infection compared to wildtype virus. In addition, the nef-deleted virus did not lead to the loss of CD4$^+$ T-cells in the periphery unlike wildtype HIV-1$_{eli}$ which led to a precipitous decline in CD4$^+$ T-cells. Taken together, our results confirm the importance of nef to *in vitro* HIV-1 viral infectivity and replication and most importantly to *in vivo* pathogenicity in this CXCR4-tropic, subtype D virus.

Materials and Methods

Humanized NSG-BLT mice

Humanized NSG-BLT mice were prepared by Jackson Laboratories. NOD/SCID IL-2γ^{null} (NSG) mice were implanted with human fetal liver and thymus, and injected intravenously with human autologous CD34 cells isolated from fetal liver. During the engraftment period, animals were maintained at University of Massachusetts in accordance to the protocols approved by the Institutional Animal Care and Use Committee. Two different human donors were used to generate 4 groups of mice used for the experiment presented in this report. The percentage of engraftment for HIV-1$_{eli\Delta nef}$ inoculated mice was 66% ± 12.6%, and for wildtype HIV-1$_{eli}$ was 67.7% ± 13.2%. Engraftment did not significantly differ between the groups. During the experimental study, NSG-BLT mice were housed and handled by BATTS laboratory (Northridge, CA) in accordance with their standard operating procedures.

Virus production and inoculation of NSG-BLT mice with HIV-1$_{eli}$ and HIV-1$_{eli\Delta nef}$

The nef-null mutation in a plasmid containing the HIV-1$_{eli}$ provirus was created by standard molecular biology techniques with the final

result being the deletion of 200 nucleotides directly downstream of the nef start codon. Nucleotides 8336-8535 were removed, as numbered in NCBI accession number K03454.1. Viral supernatants were produced after transfection of Jurkat E6-1 cells with plasmid DNA. Both HIV-1$_{eliΔnef}$ and wildtype HIV$_{eli}$ were prepared from infected Jurkat E6-1 cells. Briefly, Jurkat cells were infected at an MOI of 0.001 and then passaged every 2 days until day post-infection (dpi) 10 in RPMI-1640 containing 10% fetal bovine serum. The cell density was maintained at 1e6 cells/ml at each passage. On dpi 10, infected cells were combined with uninfected Jurkat E6-1 in a ratio of 1:3 and at a final seeding density of 2e6 cells/ml in a serum-free media; X-vivo 15 (Lonza). Viral supernatants were harvested on dpi 12 or dpi 13 and cell debris was removed by filtration through a 0.45 μm filter. Harvest material was stored frozen at -80°C until use. Aliquots of harvest material were titered using a standard TCID50 assay for 12-14 days on AA2 cells (Tissue culture infectious dose, 50%). Titers were determined after visual cytopathic effect (CPE) scoring of 16 replicates per dilution per operator and by at least 3 operators for each infectious stock used by the statistical method of Reed and Muench. Harvest supernatants were diluted with X-vivo 15 media to obtain titers of either 40,000 (4e4/ml) or 400,000 (4e5/ml) TCID50 units/ml. These diluted supernatants were then aliquoted into 0.5 ml per tube and stored at -80°C until use. The final titers in these aliquots were again tested using the TCID50 assay. Based on these titers, a final injection volume was determined for each mouse group that ranged from 210 μl to 500 μl/mouse. These frozen aliquots were shipped to BATTS Labs where they were injected intraperitoneally (IP) into the NSG-BLT mice. Four groups were injected with a total of 20,000 (2e4) or 200,000 (2e5) TCID50 units/mouse of HIV-1$_{eliΔnef}$ or HIV-1$_{eli}$. Gag-p24 concentrations were determined in duplicate with ELISA according to the manufacturer's instructions (Advance Bioscience Laboratories, Inc.).

Infection of human PBMCs

Human PBMCs were activated overnight with 5 μg/ml PHA-P (Sigma-Aldrich) in IL-2 growth media (RPMI 1640, 20% fetal bovine serum, 5% IL-2 and 50 μg/ml gentamycin). The following day cells were counted and resuspended in IL2 growth medium (without PHA-P) before being infected at an MOI of 0.001 with either HIV-1$_{eli}$ or HIV-1$_{eliΔnef}$ in 6-well dishes. Every 2 days the cells were fed with IL2 grow medium and supernatants were removed and stored at -80°C for p24 ELISA. Infections were continued for 14 days.

Virus levels in plasma

Viral RNAs in peripheral blood of infected animals were tested by real-time polymerase chain reaction (RT-PCR) assay for the integrase gene. Diluted plasma samples were sent to University of California, San Francisco (Clinical Virology Laboratory) for testing using Abbott HIV Viral Load assay. Samples were diluted 1:20 (50 μl plasma to 1 ml phosphate buffered saline), and the limit of detection was 800 RNA copies/ml. For terminal bleeds (1:5 dilution), the limit of detection was 200 copies/ml. Viral loads below the limit of detection can be detected but at less than 100% frequency.

Immunophenotyping by flow cytometry

Peripheral blood samples were immunophenotyped for human engraftments levels and monitored for CD4$^+$ and CD8$^+$ T-cell levels in infected animals. Briefly, whole blood were stained with antibodies muCD45 V450 (clone 30-F11), huCD45 APC (clone 2D11), huCD3 PE-Cy7 (clone SK7), huCD4 PE (clone SK3), huCD8 APC-H7 (clone SK1) and lysed with BD FACs lysing solution (all antibodies were from BD Biosciences). Flow cytometry was performed using a MACSQuant Analyzer 10 flow cytometer (Miltenyi) and results analyzed with FlowJo software.

Results

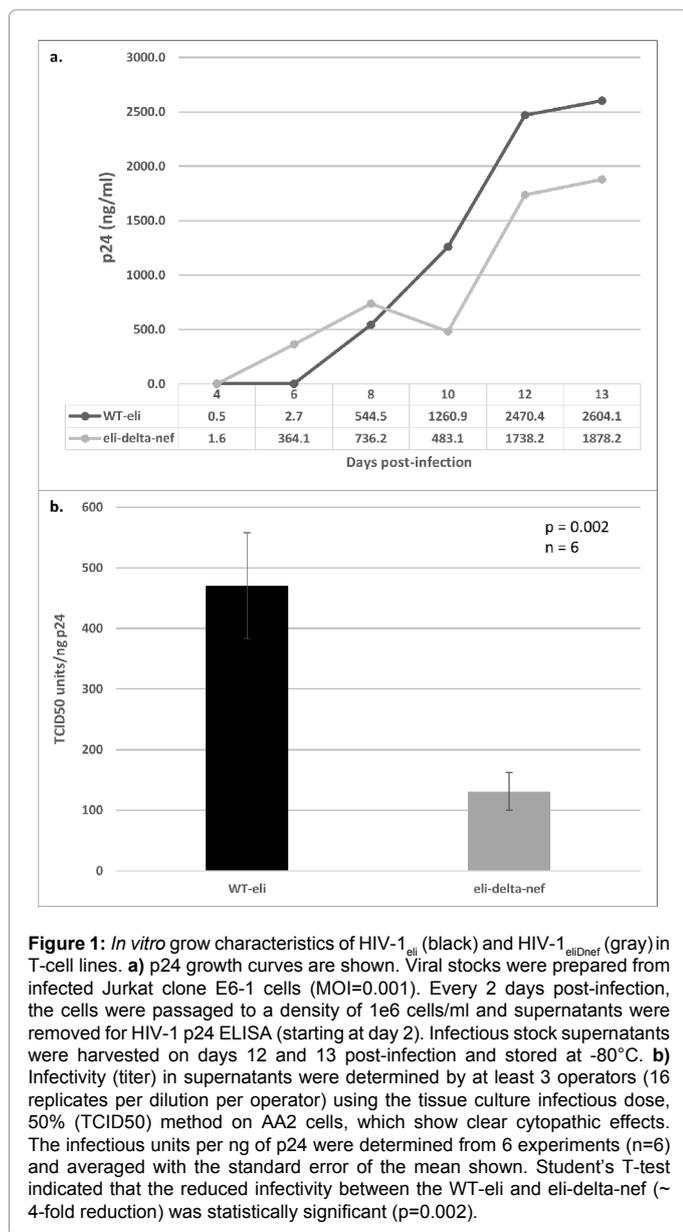### *In vitro* growth and infectivity of HIV-1$_{eli}$ and HIV-1$_{eliΔnef}$

Jurkat E6-1 cells were infected at an MOI of 0.001 with either HIV-1$_{eli}$ or HIV-1$_{eliΔnef}$. Cells were split every 2 days during which samples were removed for p24 ELISA and reseeded to a density of 1×10^6 cells/ml. Gag-p24 growth curves indicated that both viruses grew at approximately the same rate and to similar p24 levels in infected Jurkat cells (Figure 1a). TCID50 titers were determined in harvested supernatants and compared to the p24 concentrations, determined by ELISA, in order to compare infectivities between HIV-1$_{eli}$ and HIV-1$_{eliΔnef}$. Averaging the TCID50 infectious units/ng of p24 data from 6 experiments, we determined that the infectivity of the nef-deletion virus was about 4-fold reduced compared to wildtype HIV-1$_{eli}$ *in vitro* and this difference was statistically significant (Figure 1b).

We then infected activated human PBMCs from 13 different normal human donors with equal doses (MOI: 0.001) of either HIV-1$_{eli}$ or HIV-1$_{eliΔnef}$. PBMC cultures were grown for 14 days post-infection and were fed every 2 days with supernatant removed for p24 ELISA. The p24 concentrations in the supernatant were determined over 14 days and are shown in Figure 2. As expected, there was considerable variability in the p24 amounts produced by the various donor's PBMCs (Figure 2). Some donors produced higher levels of p24 than others. In PBMCs from 12 of 13 donors, there was clear evidence of viral replication; all except donor E (Figure 2a). In all other cultures, the levels of p24 were reduced when comparing wildtype HIV-1$_{eli}$ to HIV-1$_{eliΔnef}$ (Figure 2b, dark bars to light bars). These results indicate that there is a replication defect in the HIV-1$_{eliΔnef}$ virus compared to wildtype HIV-1$_{eli}$ when grown in primary human blood cells.

Infection of humanized BLT mice with HIV-1$_{eli}$ and HIV-1$_{eliΔnef}$

We injected groups of humanized BLT mice (intraperitoneal route) with 2 different infectious doses of either HIV-1$_{eli}$ or HIV-1$_{eliΔnef}$. The mice were followed for approximately 7 to 10 weeks post-injection during which viral loads and human CD4$^+$/CD8$^+$ T-cells were quantified every 2-3 weeks in peripheral blood. We did not observe significant difference in the onset of viremia between mice injected with 2×10^4 or 2×10^5 infectious units of HIV-1$_{eli}$. The same was observed for mice injected with 2×10^4 or 2×10^5 infectious units of HIV-1$_{eliΔnef}$. Therefore all mice injected with either high or low dose of HIV-1$_{eli}$ or HIV-1$_{eliΔnef}$ were grouped together.

HIV viral loads in peripheral blood were determined starting at week 1 post-injection and then every 2 weeks thereafter. For the 10 mice injected with wildtype HIV-1$_{eli}$, 6 had detectable viral loads by week 3 post-injection, 2 more at week 5, and an additional 1 by week 7 post-injection (Figure 3a). Therefore, 9 out of 10 mice injected with wildtype HIV-1$_{eli}$ eventually had detectable viremia. The average of the peaks of viremia were 2.94e5 copies/ml (± 1.6e5 copies/ml) in all mice infected with HIV-1$_{eli}$ (range of 1.46e5 to 5.4e5 copies/ml) (Figure 3a). In contrast, no mice injected with HIV-1$_{eliΔnef}$ had detectable viral loads until week 7 post-injection when 2 of 6 mice were HIV-positive (Figure 3b). At week 9 post-infection an additional mouse had detectable viremia. The average of the peaks of viremia were 4.4e3 copies/ml (± 4.5e3 copies/ml) in mice infected with HIV-1$_{eliΔnef}$ (range of 65 to 9.1e3 copies/ml) (Figure 3b). Therefore 3 out of 6 mice (50%) injected with HIV-1$_{eliΔnef}$ eventually had detectable viral loads. Comparing the

Figure 1: *In vitro* grow characteristics of HIV-1$_{eli}$ (black) and HIV-1$_{eliDnef}$ (gray) in T-cell lines. **a)** p24 growth curves are shown. Viral stocks were prepared from infected Jurkat clone E6-1 cells (MOI=0.001). Every 2 days post-infection, the cells were passaged to a density of 1e6 cells/ml and supernatants were removed for HIV-1 p24 ELISA (starting at day 2). Infectious stock supernatants were harvested on days 12 and 13 post-infection and stored at -80°C. **b)** Infectivity (titer) in supernatants were determined by at least 3 operators (16 replicates per dilution per operator) using the tissue culture infectious dose, 50% (TCID50) method on AA2 cells, which show clear cytopathic effects. The infectious units per ng of p24 were determined from 6 experiments (n=6) and averaged with the standard error of the mean shown. Student's T-test indicated that the reduced infectivity between the WT-eli and eli-delta-nef (~ 4-fold reduction) was statistically significant (p=0.002).

average peak viral loads between both groups of mice, there was a 67-fold (~1.5 to 2 log) reduction in viremia as well as an approximately 4 weeks delay in onset of viremia in the HIV-1$_{eliΔnef}$ group compared to the wildtype HIV-1$_{eli}$ group (Figure 3c).

CD4^{+} and CD8^{+} T-cells in peripheral blood samples were enumerated by flow cytometry. The ratios of human CD4^{+} to CD8^{+} T-cells were determined starting the week before injections began (week -1) and then every 1-2 weeks thereafter. All of the 9 mice that had detectable viral loads after injection of HIV-1$_{eli}$ had declining CD4^{+} T-cells in their peripheral blood over the 7 weeks post-injection (Figure 4a). Mouse #66 that did not have detectable viremia also did not show a sustained decline in CD4^{+} T-cells (Figure 4a, green line). In sharp contrast, none of the mice injected with HIV-1$_{eliΔnef}$ showed a sustained decline in CD4^{+} T-cells (Figure 4b). Comparing the average ratios of human CD4^{+} T-cell to human CD8^{+} T-cells between these 2 groups of mice it is apparent that only the wildtype HIV-1$_{eli}$ infected mice showed

rapidly declining CD4^{+} T-cell populations in the periphery but not HIV-1$_{eliΔnef}$ infected mice which had no significant sustained declines (Figure 4c).

Discussion

We have shown that deletion of nef in HIV-1$_{eli}$, a CXCR4-tropic, clade D virus produces an attenuated mutant that led to delayed viremia, lower viral loads and did not cause depletion of peripheral human CD4^{+} T-cells in infected humanized BLT mice for up to 10 weeks post-inoculation, unlike the wildtype parental virus. We also observed an infectivity defect in the nef-deletion virus produced from an immortalized T-cell line (Jurkat E6-1), as well as a replication defect in primary human immune cell cultures (PBMCs).

The *in vitro* infectivity and replication defects in HIV-1$_{eliΔnef}$ are similar to what has been described previously for clade B nef-deletion mutants in cell culture [6,9,10]. It has been known for quite some time that nef-defective viruses appear to be competent for virus production, based on p24 release, when using transformed T-cell lines [9] such as Jurkat cells, as in Figure 1a. However, the virus that is produced has an intrinsic infectivity defect as others have noted (reviewed in [6]) and as we saw in Figure 1b. The replication defect in the nef-deletion viruses has been shown to become apparent after infection of primary blood cells (PBMCs) [9], as we also observed in Figure 2.

Several studies have been reported that describe the infection of humanized BLT mice with 2 different strains of nef-deleted viruses; HIV-1$_{LAI}$ (CXCR4-tropic) and HIV-1$_{JRCSF}$ (CCR5-tropic), both of clade B origin [24-26]. The *in vivo* phenotypes observed in the humanized BLT mice infected with HIV-1$_{eli}$ and HIV-1$_{eliΔnef}$ (clade D), are different compared from what has been reported after infection of BLT mice with either wildtype HIV-1$_{LAI}$ and an LAI nef-deletion mutant or wildtype HIV-1$_{JRCSF}$ and an JRCSF nef-deletion mutant (both clade B) [24-26]. The viral loads in BLT mice infected with wildtype HIV-1$_{LAI}$ had a peak in the high e6/ml range [26] and in the mid-e6/ml range for HIV-1$_{JRCSF}$ [24] while our data show that BLT mice infected with HIV-1$_{eli}$ peaked in the low e5/ml range, a more than 1-log difference in peak viral loads compared to what has been reported. The time to maximum viremia also appeared to be faster for HIV-1$_{LAI}$ and HIV-1$_{JRCSF}$; the majority of mice taking less than 10 days, compared to the 21 days (3 weeks) post-inoculation reported in this study with wildtype HIV-1$_{eli}$ [24-26]. These differences in time of onset and maximum viremia suggest that wildtype HIV-1$_{eli}$ may be a less infectious molecular clone compared to HIV-1$_{LAI}$ and HIV-1$_{JRCSF}$ which may be a result of clade differences or are more specific to these particular strains. It is also possible that the route of inoculation caused the differences in onset of viremia; intravenous [24-26] verses intraperitoneal inoculation in this study.

The delay in onset of viremia between the nef-deletion mutant and wildtype HIV-1$_{eli}$ was also different from nef-deleted HIV-1$_{LAI}$ or HIV-1$_{JRCSF}$ [24-26]. Our results after inoculation with either 2e4 or 2e5 infectious units per mouse of HIV-1$_{eliΔnef}$ are similar to what was reported after low dose inoculation of mice with nef-deleted HIV-1$_{LAI}$ (3000 Infectious units/mouse) in that it took between 30 to 70 days to reach peak viremia but not 2 higher doses of nef-deleted HIV-1$_{LAI}$ [26]. In nef-deleted HIV-1$_{JRCSF}$ in BLT mice, there was only a few days delay in onset of viremia compared to wildtype HIV-1$_{JRCSF}$. This is in contrast to HIV-1$_{eliΔnef}$ in which viremia was delayed by about 4 weeks compared to wildtype HIV-1$_{eli}$ [24]. In addition, the maximum viral loads in the cases of nef-deleted HIV-1$_{LAI}$ or HIV-1$_{JRCSF}$ were reported to be in the mid to low e6/ml ranges respectively, while HIV-1$_{eliΔnef}$ infected mice had an average maximum viral load in the mid e3/ml range [24-26].
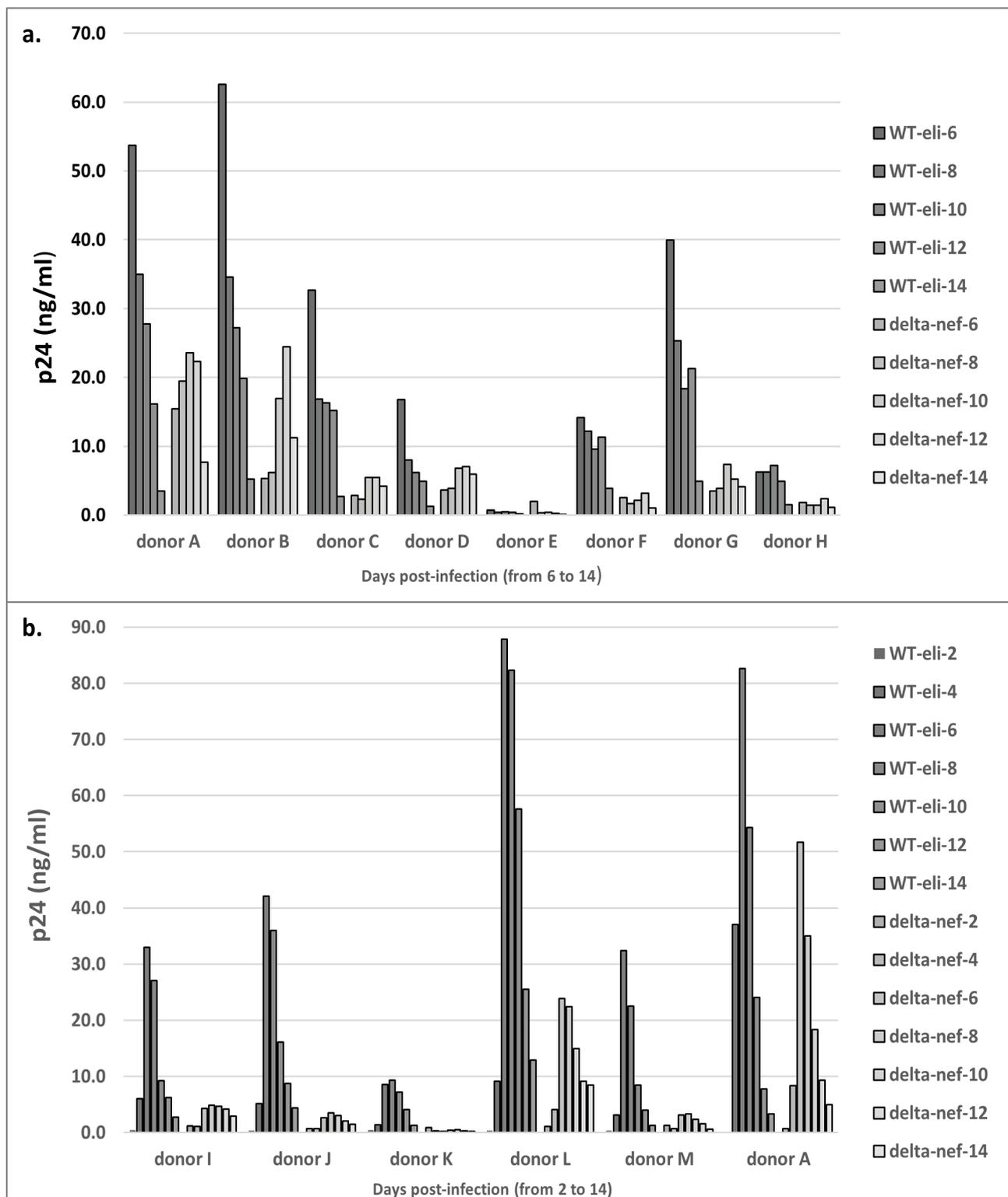
Figure 2: Replication of HIV-1eli (WT-eli; darker bars) and HIV-1eliDnef (delta-nef; lighter bars) in human PBMCs up to 14 days post-infection from 13 different donors in 2 independent experiments. PBMCs were activated with PHA overnight before infection with either virus (MOI: 0.001). **a)** Supernatants were removed every 2 days for p24 ELISA before fresh media was added starting on dpi 6. **b)** Supernatants were removed every 2 days for p24 ELISA before fresh media was added starting on dpi 2. In 12 of the 13 donors, wildtype HIV-1eli replicated to higher levels than HIV-1eliDnef based on p24 levels in the supernatant. Neither virus replicated to appreciable levels in PBMCs from donor E.
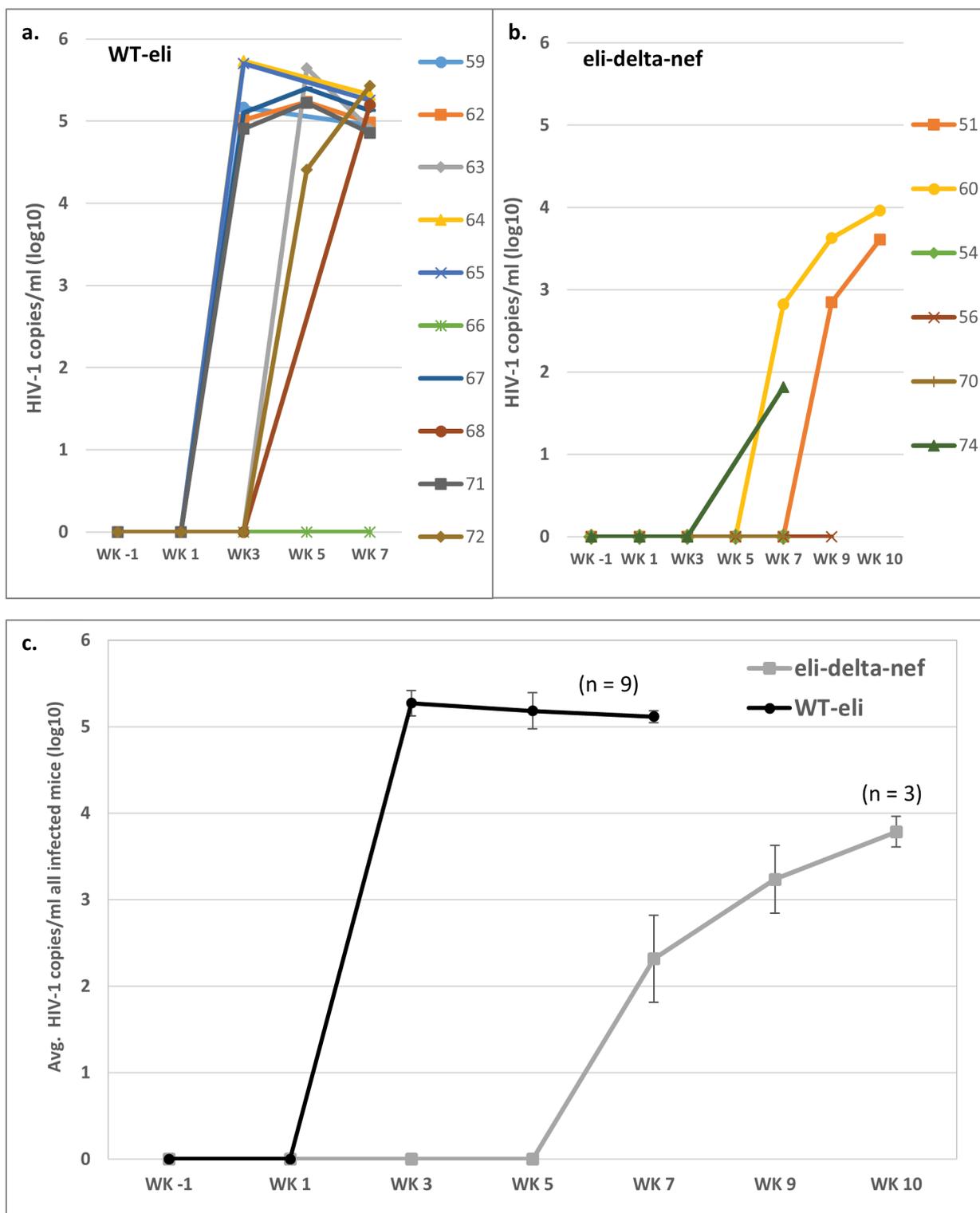
Figure 3: Viremia in BLT mice injected with HIV-1$_{eli}$ (WT-eli) or HIV-1$_{eliDnef}$ (eli-delta-nef). **a)** HIV-1 viral loads (in log10 scale) in the peripheral blood of 10 BLT mice injected with HIV-1$_{eli}$ are shown to 7 weeks post-injection. Only mouse #66 (green) did not have a detectable viral load up to week 7. **b)** HIV-1 viral loads (in log10 scale) in the peripheral blood of 6 BLT mice injected with HIV-1$_{eliDnef}$ are shown up to 10 weeks post-injection. Three mice had detectable viral loads (#51, 60 & 74) while 3 did not (#54, 56 & 70). **c)** The viral loads in all mice displaying detectable viremia were averaged to compare average levels of viremia between the HIV-1$_{eli}$ and HIV-1$_{eliDnef}$ groups. Error bars indicate the standard error of the mean.
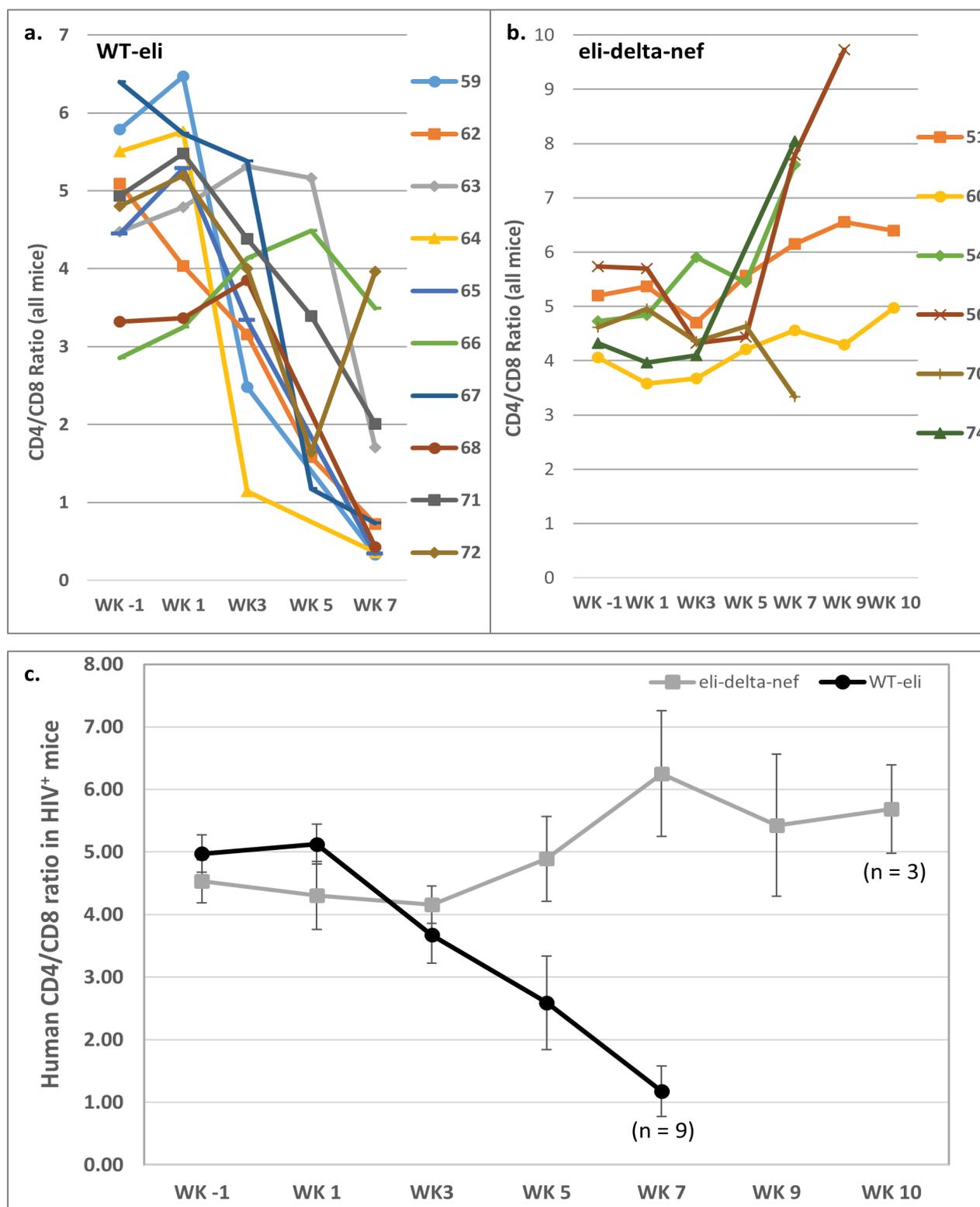
Figure 4: Peripheral CD4 T-cells in BLT mice injected with HIV-1$_{eli}$ (WT-eli) or HIV-1$_{eliDnef}$ (eli-delta-nef). **a)** The ratio of human CD4 to CD8 T-cells in the peripheral blood of 10 BLT mice injected with HIV-1$_{eli}$ are shown to 7 weeks post-injection. Mouse #66 (green) did not have detectable viral loads up to week 7 and did not show a decline in CD4 T-cells. **b)** The ratio of human CD4 to CD8 T-cells in the peripheral blood of 6 BLT mice injected with HIV-1$_{eliDnef}$ are shown up to 10 weeks post-injection. None of the mice had a sustained drop in CD4 T-cells. **c)** The human CD4 to CD8 ratio in all mice displaying detectable viremia were averaged to compare average levels of CD4 T-cell loss between the HIV-1$_{eli}$ and HIV-1$_{eliDnef}$ groups. Error bars indicate the standard error of the mean.

The mechanistic reasons for these differences in peak viremia between HIV-1 strains are not known.

Conclusion

Our results are in agreement with the idea that nef is a critical factor in determining the pathogenesis of HIV-1. We have shown that HIV-1$_{eli}$ nef is necessary for high plasma viral loads and for depletion of peripheral CD4$^+$ T-cells in this advanced animal model of HIV disease. These results indicate that HIV-1$_{eli\Delta nef}$ is a pathogenically-attenuated mutant of HIV-1$_{eli}$ and may be useful for further vaccine development.

References

1. Goldsmith MA, Warmerdam MT, Atchison RE, Miller MD, Greene WC (1995) Dissociation of the CD4 downregulation and viral infectivity enhancement functions of human immunodeficiency virus type 1 Nef. J Virol 69: 4112-4121.

2. Landi A, Iannucci V, Van Nuffel A, Meuwissen P, Verhasselt B (2011) One protein to rule them all: modulation of cell surface receptors and molecules by HIV Nef. Curr HIV Res 9: 496-504.

3. Hrecka K, Swigut T, Schindler M, Kirchhoff F, Skowronski J (2005) Nef proteins from diverse groups of primate lentiviruses downmodulate CXCR4 to inhibit migration to the chemokine stromal derived factor 1. J Virol 79: 10650-10659.

4. Michel N, Allespach I, Venzke S, Fackler OT, Keppler OT (2005) The Nef protein of human immunodeficiency virus establishes superinfection immunity by a dual strategy to downregulate cell-surface CCR5 and CD4. Curr Biol 15: 714-723.

5. Schwartz O, Maréchal V, LeGall S, Lemonnier F, Heard JM (1996) Endocytosis of major histocompatibility complex class I molecules is induced by the HIV-1 Nef protein. Nat Med 2: 338-342.

6. Vermeire J, Vanbillemont G, Witkowski W, Verhasselt B (2011) The Nef-infectivity enigma: mechanisms of enhanced lentiviral infection. Curr HIV Res 9: 474-489.

7. Olivieri KC, Mukerji J, Gabuzda D (2011) Nef-mediated enhancement of cellular activation and human immunodeficiency virus type 1 replication in primary T cells is dependent on association with p21-activated kinase 2. Retrovirology 8: 64.

8. Trible RP, Emert-Sedlak L, Smithgall TE (2006) HIV-1 Nef selectively activates Src family kinases Hck, Lyn, and c-Src through direct SH3 domain interaction. J Biol Chem 281: 27029-27038.

9. Miller MD, Warmerdam MT, Gaston I, Greene WC, Feinberg MB (1994) The human immunodeficiency virus-1 nef gene product: a positive factor for viral infection and replication in primary lymphocytes and macrophages. J Exp Med 179: 101-113.

10. Pizzato M, Helander A, Popova E, Calistri A, Zamborlini A, et al. (2007) Dynamin 2 is required for the enhancement of HIV-1 infectivity by Nef. Proc Natl Acad Sci USA 104: 6812-6817.

11. Foster JL, Garcia J (2008) HIV-1 Nef: at the crossroads. Retrovirology 5: 84.

12. Churchill MJ, Rhodes DI, Learmont JC, Sullivan JS, Wesselingh SL, et al. (2006) Longitudinal analysis of human immunodeficiency virus type 1 nef/long terminal repeat sequences in a cohort of long-term survivors infected from a single source. J Virol 80: 1047-1052.

13. Gorry PR, McPhee DA, Verity E, Dyer WB, Wesselingh SL, et al. (2007) Pathogenicity and immunogenicity of attenuated, nef-deleted HIV-1 strains in vivo. Retrovirology 4: 66.

14. Greenough TC, Sullivan JL, Desrosiers RC (1999) Declining CD4 T-cell counts in a person infected with nef-deleted HIV-1. N Engl J Med 340: 236-7.

15. Kondo M, Shima T, Nishizawa M, Sudo K, Iwamuro S, et al. (2005) Identification of attenuated variants of HIV-1 circulating recombinant form 01_AE that are associated with slow disease progression due to gross genetic alterations in the nef/long terminal repeat sequences. J Infect Dis 192: 56-61.

16. Rhodes DI, Ashton L, Solomon A, Carr A, Cooper D, et al. (2000) Characterization of three nef-defective human immunodeficiency virus type 1 strains associated with long-term nonprogression. Australian Long-Term Nonprogressor Study Group. J Virol 74: 10581-10588.

17. Salvi R, Garbuglia AR, Di Caro A, Pulciani S, Montella F, et al. (1998) Grossly defective nef gene sequences in a human immunodeficiency virus type 1-seropositive long-term nonprogressor. J Virol 72: 3646-3657.

18. Skowronski J, Parks D, Mariani R (1993) Altered T cell activation and development in transgenic mice expressing the HIV-1 nef gene. EMBO J 12: 703-713.

19. Kestler HW, Ringler DJ, Mori K, Panicali DL, Sehgal PK, et al. (1991) Importance of the nef gene for maintenance of high virus loads and for development of AIDS. Cell 65: 651-662.

20. Kirchhoff F, Schindler M, Specht A, Arhel N, Münch J, et al. (2008) Role of Nef in primate lentiviral immunopathogenesis. Cell Mol Life Sci 65: 2621-2636.

21. Peden K, Emerman M, Montagnier L (1991) Changes in growth properties on passage in tissue culture of viruses derived from infectious molecular clones of HIV-1LAI, HIV-1MAL, and HIV-1ELI. Virology 185: 661-672.

22. Ito R, Takahashi T, Katano I, Ito M (2012) Current advances in humanized mouse models. Cell Mol Immunol 9: 208-214.

23. Yamada E, Yoshikawa R, Nakano Y, Misawa N, Koyanagi Y, et al. (2015) Impacts of humanized mouse models on the investigation of HIV-1 infection: illuminating the roles of viral accessory proteins in vivo. Viruses 7: 1373-1390.

24. Watkins RL, Foster JL, Garcia JV (2015) In vivo analysis of Nef's role in HIV-1 replication, systemic T cell activation and CD4(+) T cell loss. Retrovirology 12: 61.

25. Watkins RL, Zou W, Denton PW, Krisko JF, Foster JL, et al. (2013) In vivo analysis of highly conserved Nef activities in HIV-1 replication and pathogenesis. Retrovirology 10: 125.

26. Zou W, Denton PW, Watkins RL, Krisko JF, Nochi T, et al. (2012) Nef functions in BLT mice to enhance HIV-1 replication and deplete CD4+CD8+ thymocytes. Retrovirology 9: 44.